

See discussions, stats, and author profiles for this publication at: <https://www.researchgate.net/publication/343547414>

Tempo-spatial Pattern of Wind Speed and Urban Stilling Island in Beijing City

Article in *Journal of Meteorological Research* · August 2020

DOI: 10.1007/s13351-020-9135-5.

CITATIONS

0

READS

26

4 authors, including:



Guoyu Ren

China Meteorological Administration, Beijing; China University of Geosciences, Wuhan

288 PUBLICATIONS 6,523 CITATIONS

SEE PROFILE

Some of the authors of this publication are also working on these related projects:



Change in extreme climate over East Asian Monsoon Region (EAMR) [View project](#)



International Atmospheric Circulation Reconstructions over the Earth (ACRE) China [View project](#)

Tempo–spatial Pattern of Wind Speed and Urban Stilling Island in Beijing City

Ping YANG, Guoyu REN, Pengcheng YAN, Jingmian DENG

Citation: Ping YANG, Guoyu REN, Pengcheng YAN, Jingmian DENG, 2020. Tempo–spatial Pattern of Wind Speed and Urban Stilling Island in Beijing City, *Journal of Meteorological Research*, 34, 1–11. doi: [10.1007/s13351-020-9135-5](https://doi.org/10.1007/s13351-020-9135-5).

View online: <http://www.jos.ac.cn/article/shaid/04d758067e3e4a4b1ef4ab65db63a3e94cd53eaeef76e5d4eb3c979e1ec136b2>

Related articles that may interest you

[Spatial and Temporal Variability of Surface Wind Speed during 1961–2017 in the Jing–Jin–Ji Region, China](#)

Journal of Meteorological Research. 2020, (), <https://doi.org/10.1007/s13351-020-9119-5>

[Urban Heat Island Investigations in Arctic Cities of Northwestern Russia](#)

Journal of Meteorological Research. 2017, 31(6), 1161 <https://doi.org/10.1007/s13351-017-7048-8>

[Below–Cloud Aerosol Scavenging by Different–Intensity Rains in Beijing City](#)

Journal of Meteorological Research. 2019, 33(1), 126 <https://doi.org/10.1007/s13351-019-8079-0>

[Advances in Urban Meteorological Research in China](#)

Journal of Meteorological Research. 2020, 34(2), 218 <https://doi.org/10.1007/s13351-020-9858-3>

[Characteristics of Boundary Layer Structure during a Persistent Haze Event in the Central Liaoning City Cluster, Northeast China](#)

Journal of Meteorological Research. 2018, 32(2), 302 <https://doi.org/10.1007/s13351-018-7053-6>

[Regional Meteorological Patterns for Heavy Pollution Events in Beijing](#)

Journal of Meteorological Research. 2017, 31(3), 597 <https://doi.org/10.1007/s13351-017-6143-1>

Tempo-spatial Pattern of Wind Speed and Urban Stilling Island in Beijing City

Ping YANG^{1,3}, Guoyu REN^{2,4*}, Pengcheng YAN⁵, and Jingmian DENG¹

¹ China Meteorological Administration (CMA) Training Center, Beijing 100081

² Department of Atmospheric Science, School of Environmental Studies, China University of Geosciences, Wuhan 430000

³ Institute of Urban Meteorology, CMA, Beijing 100081

⁴ Laboratory for Climate Studies, National Climate Center, CMA, Beijing 100081

⁵ Institute of Arid Meteorology, China Meteorological Administration, Lanzhou 730000

(Received December 4, 2019; in final form April 7, 2020)

ABSTRACT

An hourly-resolution dataset of Beijing's automatic weather stations (AWSs) is developed and applied to study the characteristics of weakening wind in urban area. Urban Stilling Island (USI) is presented in this paper to discuss the wind speed (WS) differences between urban and rural regions. The urban sites are referring to the 45 stations within the 6th Ring Road (RR), while another six stations outside the built-up areas are selected as rural sites. The period for study is from 2008 to 2017. The results demonstrate a remarkable smaller annual and seasonal average WS in built-up areas compared to rural areas, which can be explained by the continuous urbanization and higher buildings in urban areas. The USI phenomenon has been visible in urban areas, especially in central urban areas (within the 4th RR). In this case, concentrated buildings may play a crucial role. It is closely related to the faster large-scale flow in spring and winter, which is dominated by the surface roughness effect. The diurnal USI intensity (USII) variations are characterized by a steadily low USII stage from 1900 to 0800 Beijing Time (BT) and a high USII stage from 1100 to 1500 BT. The rapid shifts of USII values from low to high, and from high to low, occur during the periods of 0800-1100 and 1500-1900 BT respectively. The strongest USII appears during the daytime (0800-1600) in springtime. Daily variation of USII is mainly attributed to solar radiation.

Key words: wind speed (WS), urban stilling island (USI), climatology, Beijing city

Citation: Yang, P., G. Y. Ren, P. C. Yan, et al., 2020: Tempo-spatial pattern of wind speed and urban stilling island in Beijing city. *J. Meteor. Res.*, **34**(x), 1–11, doi: 10.1007/s13351-020-9135-5.

1. Introduction

Wind is one of the most direct and exiguous climatic elements affecting the daily life of mankind. It is closely associated with air pollution, sand storms, wind power generation, sailing race and so on (Pielke et al., 2002). Wind speed (WS), as an important indicator of wind field, is very essential to many other climatic variables. Firstly, WS is a main factor affecting evapotranspiration, which is a key process of the climate and water cycle change at land surface (Hobbins et al., 2004). Secondly, WS affects the accuracy of the observation data of precipitation. The higher WS often lowers the catch-rate (under-catch) of precipitation (Yang et al., 1999; Zheng and Ren, 2017). Thirdly, WS is also an indispensable

part of urban climatology, affecting Urban Heat Island (UHI), air pollution and hydro-process (Hou et al., 2013).

Previous studies have found that, UHI is usually weaker in windy season (Unger, 1996; Alonso et al., 2007; Yang et al., 2013). As a key urban climatic indicator, the characteristics of UHI and its causes have been discussed by many scholars (e.g. Oke, 1988; Ren et al., 2005, 2007; Yang et al., 2013; Ren and Zhou, 2014; Bian et al., 2018, Shapiro and Fedorovich, 2018). In fact, WS, precipitation, humidity, air pollution, et al., are other important urban climatic indicators that are remarkably different in urban areas from those in rural areas (Ashrafi et al., 2009; Cuadrat et al., 2015, Yang et al., 2017; Chai et al., 2018).

Many studies have demonstrated that the WS shows a

This study is financially supported by the Ministry of Science and Technology of China (2018YFA0606302) and China Natural Science Foundation (41775078, 41675092, and 41575003).

*Corresponding author: guoyoo@cma.gov.cn.

©The Chinese Meteorological Society and Springer-Verlag Berlin Heidelberg 2020

decreasing trend over the past decades in countries like China, Austria, Canada, Europe, and America (e.g. Klink, 1999; Pirazzoli and Tomasin, 2003; Tuller, 2004; Xu et al., 2006; Roderick et al., 2007; Azorin-Molina et al., 2016; Yao and Li, 2016; Torralba et al., 2017). In some high latitude countries, however, opposite conclusions are drawn (Lynch et al., 2004; Aristidi, 2005; Turner et al., 2005). China is a country situated in the middle and low latitudes. Numerous researches shows that WS in China has weakened remarkably, especially in the northern parts of the country (Jiang et al., 2010, Li et al., 2011; Hou et al., 2013), and this phenomenon may be related to three factors: global warming, weakening monsoons and rapid urbanization. The first two reasons have been already discussed by many researchers (Zhang et al., 2014; Wu and Wu, 2016).

There are some observational evidence of relationship between WS change and urbanization in the past, but the analyses are still insufficient. One of the commonly recognized phenomenon is that the near surface WS in city is different from that in rural areas, due to the special thermal and dynamic properties of land surface in urban areas (Robert and Johnson, 1977). In many cities of China, such as Beijing, Lanzhou, Nanjing, Wuhan, and Shanghai, the annual and seasonal mean WS in cities are lower than that in their rural sites (Liu et al., 2002; Miao et al., 2016; Wu and Wu, 2016). It is also recognized that higher WS is helpful to the diffusion of atmospheric pollutants (Hosler, 1961; Ashrafi et al., 2009). For example, it has been concluded that high WS is one of the dominant influences to air pollution in Washington and Oregon coastal areas (Ashrafi et al., 2009). Besides, some pieces of evidence shows that WS exceeding a threshold value could prevent the development of UHIs (Alonso et al., 2007).

However, the previous studies of WS mostly focuses on the local phenomenon in large spatial-temporal scale instead of the detailed contrast between city and rural areas due to the insufficient high-density observations. During the past several years, many automatic weather stations (AWSs) have been built up in China. All the construction of AWSs meets the operational standards set by the China Meteorological Administration (CMA). By 2017, for example, a dense AWS network of about 200 stations has been developed in Beijing area (Yang et al., 2011, 2013, 2017). About two-thirds of the stations of the network are able to provide the observations of hourly mean WS.

In this paper, the hourly mean WS data obtained by AWSs in Beijing are applied to investigate the climatological tempo-spatial pattern of WS. We also make a com-

parison of WS in urban and rural areas by calculating the WS difference between the rural stations and urban stations, which is named as Urban Stilling Island (USI) in this paper. In the following sections, information and basic climatological features of WS in urban area in Beijing during 2008-2017 will be illustrated first; then we will examine the detailed features of USI intensity (USII) in built-up areas, including the spatial distribution, diurnal cycle and seasonal variation; last but not least, the reason for the USII variation will be discussed briefly before the conclusions.

2. Data and methods

Beijing City, located in the north of the North China Plain and south to the Yan Shan Mountains, covers an area of almost 1.6 million square kilometers. The flat southeast region in Beijing is occupying roughly 38%, while the rest northwest area is mostly mountainous. Beijing has a typical monsoon-driven semi-humid continental climate. It is hot in summer and cold in winter, and enjoys a seasonally high concentrated summer precipitation regime. Since the 1980s, Beijing has experienced rapid urbanization. Up to 2007, the urbanized regions have expanded and covered a much larger area than that of the 1980s. So far, a multi Ring Road (RR) system of transportation (Fig. 1) has been developed in the urban zones (Mu et al., 2012; Yang et al., 2013), and the 4th, 5th, and 6th RRs came into service in 2001, 2003, and 2009, successively. This analysis will be focused on the urban area (inside the 6th RR).

Hourly WS data of 160 autonomous weather stations (AWS) over Beijing for the time period 2008-2017 are

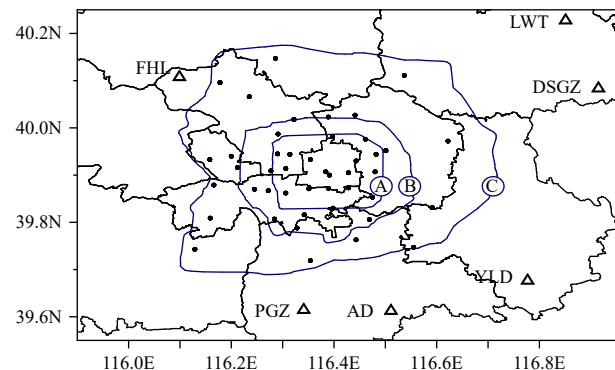


Fig. 1. Stations in the Beijing urban region outlined within the 6th Ring Road (RR; blue solid circles; lines A, B, and C represents 4th RR, 5th RR, and 6th RR respectively) and the six rural stations outside of the 6th Ring Road (Abbreviations of the station names are FHL for Feng Huang Ling, YLD for Yong Le Dian, PGZ for Pang Ge Zhuang, AD for An Ding, DSGZ for Da Sun Ge Zhuang, and LWT for Long Wan Tun).

obtained from the Meteorological Information Center, Beijing Meteorological Bureau (MIC/BMB). A quality-control process developed by Yang et al. (2011) is adopted in order to ensure the validity of the high-density AWS data. The stations with over 3% of missing records have been taken out directly, and the questionable records have been checked and corrected through regionally climatic extreme-value thresholds (Yang et al., 2013). Finally, 45 observation stations are selected as urban stations, which are relatively evenly located inside 6th RR, in addition to six rural stations outside the 6th RR (Fig. 1).

In this paper, the satellite remote-sensing technology is also applied in rural station selection. The brightness temperature is obtained from MODIS dataset first, and then the temperature isolines surrounding the stations will be drawn in order to compare the WS of urban and rural sites. (Ren and Ren 2011; Yang et al., 2013, 2017). Finally, six rural stations are selected. All the selected rural stations have similar natural characteristics with those urban observational sites. In particular, their average altitude are almost the same and their locations are quite close to the urban areas. The detailed information of the six stations is shown in Table 1.

In this study, the USII is defined as the WS difference between one or several urban sites and rural areas. The rural WS (WS_r) refers to the mean value of WS of the six reference stations outside the urban areas, while the urban WS (WS_u) means the WS of any urban station, or the mean WS of certain types of urban stations. The USII (ΔWS_{r-u}) can be thus defined as:

$$USII = -WS_{u-r} = (WS_r - WS_u), \quad (1)$$

The significance testing is used for the difference of mean WS between urban and rural stations, and the difference is considered statistically significant if it is at the 95% ($P < 0.05$) confidence level.

3. Features of mean WS

3.1 Spatial characteristics

Figure 2 shows the spatial distributions of annual mean WS in the study area of Beijing. The contour maps with interpolated grid values used in this paper are drawn

with Kriging Methods. During the ten-year period, the annual mean WS of the whole study region is 1.11 m s^{-1} , which is 0.21 m s^{-1} slower than that of rural stations (annual mean WS of six rural stations is 1.32 m s^{-1} , and Table 2 shows the annual mean WS of each rural station). The site-to-site difference between the maximum and minimum annual mean WS values is 1.58 m s^{-1} . The lowest value (0.46 m s^{-1}) is obtained from Beijing Workers' Stadium (BWS; Fig. 2) inside the 4th RR (annual mean WS inside the 4th RR is 0.92 m s^{-1}), while the highest one (2.04 m s^{-1}) is recorded by Beijing Observatory (BO; Fig. 2) near the 5th RR. As a national station of Beijing, BO is in compliance strictly with the highest standards for observational environment, which requires quite open surroundings. Thus, the faster air flow caused by the open space around BO could be the main reason for the higher WS record.

Figure 2 also shows that the annual mean WSs in the east and south show generally higher values. Obviously, this large spatial difference of the annual mean WS values mainly results from USI effects, which lead to a significant decrease in the WS over built-up areas.

3.2 Temporal characteristics

The temporal characteristics of hourly and pentad mean WS in urban and rural areas are shown in Figs. 3a, b. Blue lines in the figure represent 1.0 m s^{-1} isolines of mean WS, while red lines represent 2.4 m s^{-1} isolines of mean WS. It is obvious that the temporal patterns of WSs are similar between urban and rural areas, and the wind force in rural area is a little bit larger. The WS experiences a smaller diurnal variation in autumn compared to other seasons. For example, the daily range of hourly mean WS in urban area (Fig. 3a) is within 0.88 m s^{-1} in autumn, while in spring it can reach to 1.48 m s^{-1} .

Figure 3 also indicates that the WS shift between night and day is large in spring and small in autumn. The high-values in both urban and rural region occur at daytime in spring and winter while the low-values lie in the period from midnight to early morning. Besides, the considerable differences exist between the urban and rural areas. A significance test is taken to examine the WS difference between the urban and rural stations. For time series

Table 1. Basic information of six rural stations

Abbrev. (name)	Lon. (E)/Lat. (N)	Elevation (m)	Elevation difference from urban areas (m)
FHL (Feng Huang Ling)	116.10°/40.11°	73.0	26.1
YLD (Yong LeDian)	116.78°/39.68°	17.0	-29.9
PGZ (Pang Ge Zhuang)	116.34°/39.62°	34.0	-12.9
AD (An Ding)	116.51°/39.62°	24.0	-22.9
DSGZ (Da Sun Ge Zhuang)	116.92°/40.09°	35.0	-11.9
LWT (Long Wan Tun)	116.85°/40.23°	52.0	5.1
Average	116.51°/39.90°	39.2	-7.7

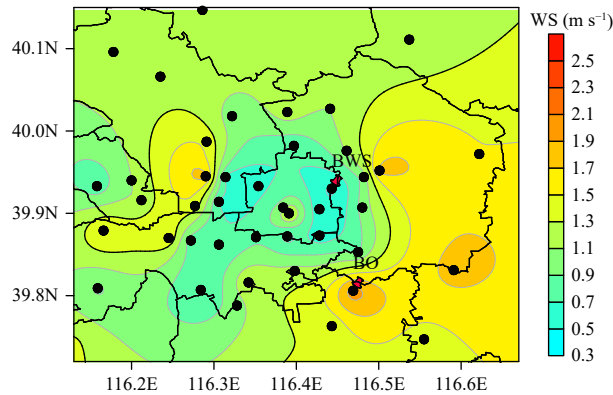


Fig. 2. Spatial distributions of annual mean values of WS in Beijing study area during 2008-2017.

of hourly average values and pentad average values, the t values are 41.13 and -3.92 respectively, both of which pass the confidence level of 0.001. In the rural area, the maximum hourly mean WS can reach to 3.7 m s^{-1} (16 h, 23 pentad) during the strong WS stage in spring, approximately 3.0 m s^{-1} higher than the smallest hourly mean WS of 0.8 m s^{-1} (4 h, 44 pentad) recorded during the weak WS stage in summer. By comparison, the difference between the highest and the lowest hourly mean WS in urban areas does not exceed 2.5 m s^{-1} . Once again, the area where hourly mean WS exceeds 2.4 m s^{-1} (red line) at daytime in rural area is much larger than that in urban area, while the region where the WS values less than 1.0 m s^{-1} in rural areas turns out to be smaller than that in urban area. Obviously, the diurnal variation of WS among different seasons in rural areas is generally larger than those in urban areas.

It is known that the WS has been influenced largely by urbanization and the higher buildings around observational sites (e.g. Landsberg, 1956; Yu et al., 2014; Bian et al., 2018). Making use of the dense dataset, the apparent differences of WS value can also be found in this work. Surface roughness is obviously one of the most important factors. In the urban center, because of the buildings increased both in density and height (Ge et al., 2016), the underlying surfaces have been evolved from relatively heterogeneity to roughness, and the distribution of flow field have changed fundamentally (Peng and Hu, 2006). Consequently, the mean WS in urban areas, especially in urban center, has been decreased significantly.

4. Tempo-spatial pattern of USII

4.1 Spatial distribution of USII

Figure 4 demonstrates the spatial pattern of the annual

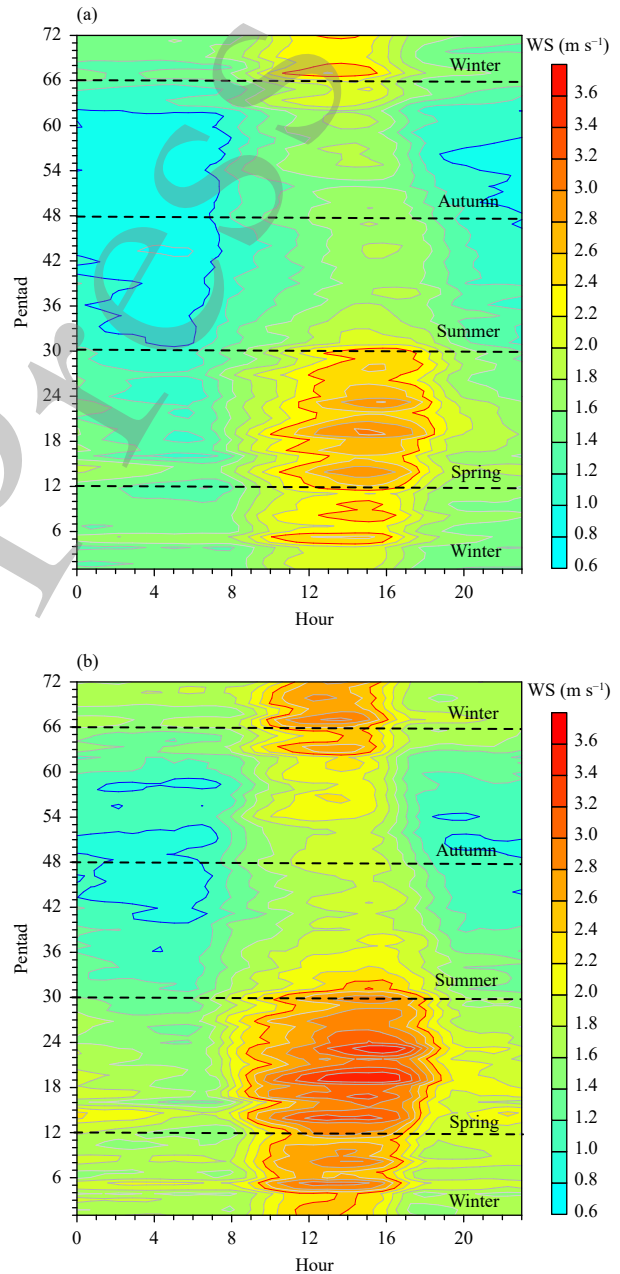


Fig. 3. Hour-pentad profile of mean value of WS for urban area (a) and rural area (b) during 2008-2017. Blue lines represent 1.0 m s^{-1} isolines of mean value of WS while red lines represent 2.4 m s^{-1} isolines of mean value of WS.

average USII inside urban areas. The maximum USII center (0.86 m s^{-1}) appears at BWS, which coincides with the annual mean high-WS value in Fig. 2. The largest USII values, 0.5 m s^{-1} (marked by pink lines) or greater, mostly occur within the 4th RR. In fact, the annual mean USII value inside the 4th RR is 0.52 m s^{-1} . Tian'anmen (TAM; Fig. 4) is the only station that recorded a low USII value (0.17 m s^{-1}) inside the 4th RR, which is located in the most urbanized center of Beijing

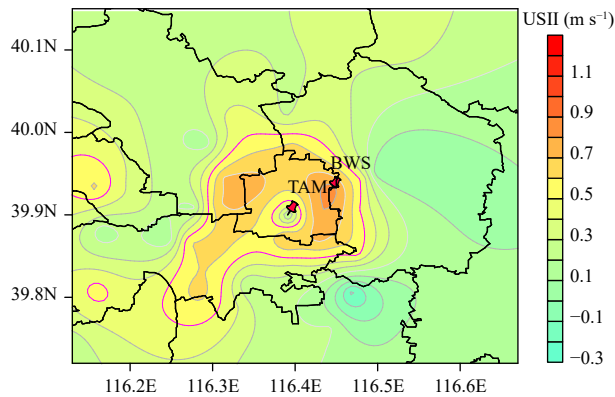


Fig. 4. Spatial distributions of annual mean values of USII (m s^{-1}) in urban area over Beijing during 2008-2017. Pink lines represent 0.5 m s^{-1} isolines of mean value of USII.

City. This phenomenon can be explained by the open surroundings of the site. The most spacious urban square in the world, TAM Square, is next to the site, and several large parks are also located around TAM, such as Zhongshan Park, Beihai Park, Jingshan Park and so on. Previous study has also illustrated that the concentrated trees and grass in parks in urban areas help to weaken the

UHI effect (e.g. Yang et al., 2016). Ge et al. (2016) also found that high and dense buildings weaken WS, while dispersed buildings with larger open space help to keep airflow moving. Therefore, the apparent low USII value recorded by TAM is more likely caused by the open space around the observational site.

Figure 5 demonstrates the spatial pattern of the seasonal average USII values in Beijing's urban areas. As is shown, the area enclosed by the pink isoline of 0.5 m s^{-1} is larger in Figs. 5a, d than the other two panels, indicating that the USIIs are stronger in spring and winter. The USIIs in spring are the strongest as more than half of the sites (21 sites) have the records of over 0.5 m s^{-1} , which can be seen clearly in Fig. 5a. The only low record in urban center is still from TAM site, which is only 0.24 m s^{-1} of seasonal mean value. In contrast, the seasonal mean USII is a little weaker in winter as the 0.5 m s^{-1} isoline circles a narrower area (Fig. 5d). Although the low-value areas of TAM in urban center still exist, the value of USII is a little larger than that in spring (0.35 m s^{-1}). Furthermore, the USIIs in spring demonstrate a more remarkable spatial difference than in winter. The

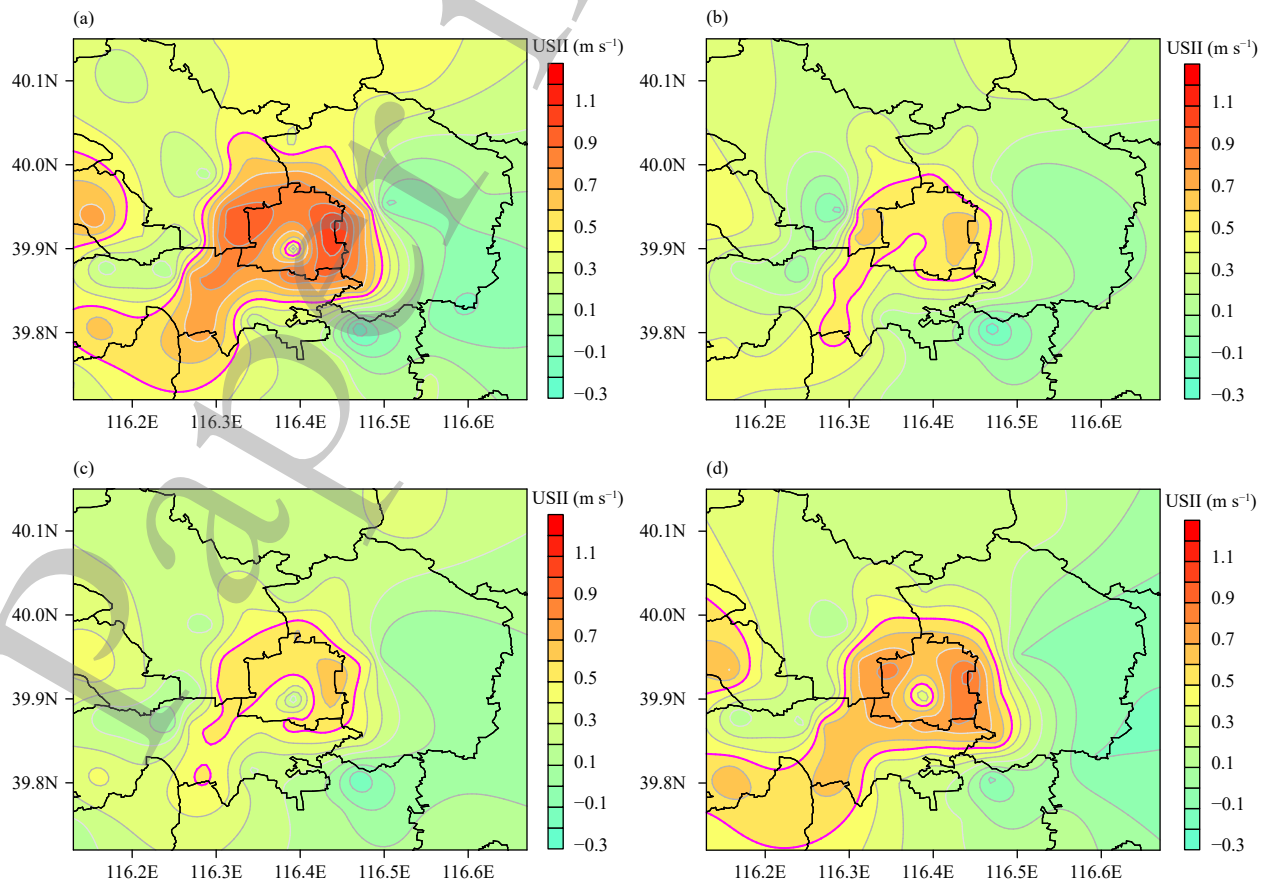


Fig. 5. Spatial distributions of seasonal [(a) spring, (b) summer, (c) autumn, and (d) winter] mean values of USII (m s^{-1}) in urban area over Beijing during 2008-2017. Pink lines represent 0.5 m s^{-1} isolines of mean value of USII.

spatial patterns of seasonal mean USII in summer and in autumn are similar. Both of their average values of USII are 0.35 and the 0.5 m s^{-1} isolines cover a small area in or around the 4th RR. However, there is an additional area enclosed by 0.5 m s^{-1} isoline around southwest of the 4th RR, as shown in Fig. 5b, indicating that the seasonal mean USII is slightly higher in summer than in autumn.

4.2 Temporal characteristics of USII

Figure 6 displays the diurnal variation of annual and seasonal mean USII in Beijing city during 2008-2017. The variations of both annual and seasonal values are similar. The maximum USII value occurs in the noon while the minimum one comes at the sunset. The diurnal curve of annual mean USII demonstrates that the USII value remains low from evening [1800 Beijing Time (BT)] to the next morning (0700 BT), and it keeps high for only 4-5 h. The rest of a day can be considered as swift-changing stages, including a surge stage (0700-1100 BT) and a sharp decline stage (1500-1800 BT). In addition, the spatial distributions of USII during periods of daytime (0700-1800 BT) and nighttime (1900-0600 BT) are both analyzed, which are similar to Fig. 4, demonstrating a larger value of USII inside the 4th RR.

Although the diurnal curves are similar in the whole year, the seasonal differences still exist. Firstly, in spite of the similar appearance time of valley values (1800 or 2000 BT), the peaks time are almost different in each season, which are 1000, 1200, 1100, and 1200 BT in spring, summer, autumn and winter respectively (Fig. 6 and Table 2). It is evident that the USI effects remain weak from evening to next early morning (1900 to 0800 BT), and the largest seasonal hourly mean value of USII

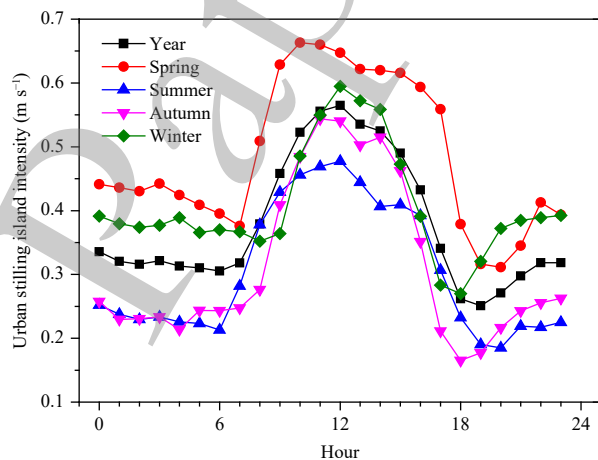


Fig. 6. Diurnal variation of annual and seasonal mean USII in urban area of Beijing during 2008-2017.

Table 2. Annual mean WS of each rural station. Unit: m s^{-1} (See Fig. 1 for the abbreviations of the rural station names)

	FHL	YLD	PGZ	AD	DSGZ	LWT	Average
WS	1.42	1.54	1.48	1.26	1.14	1.13	1.32

is no more than 0.45 m s^{-1} during this time. Secondly, the seasonal mean USII varies in different seasons. Table 2 and Figure 6 show that the strongest USII occurs in spring, and the second strongest USII occurs in winter, while summer and autumn see relatively weaker USII values. Thirdly, the diurnal ranges of the hourly average USII values witness an inter-seasonal difference. The smallest USII diurnal range appears in winter while autumn sees a greater diurnal variation.

Month-year and hour-year profiles of hourly average USII are demonstrated in Fig. 7. In Fig. 7a, it is clear that the whole stage from 2008 to 2017 can be considered in two separate intervals, which are the period with larger USII values (2008 to 2012) and the period with smaller USII values (2013 to 2017). The reason for the change may be related to the weak background near-surface WS, but the details need to be further investigated. The low-layer circulation weakened since 2013, which decreased

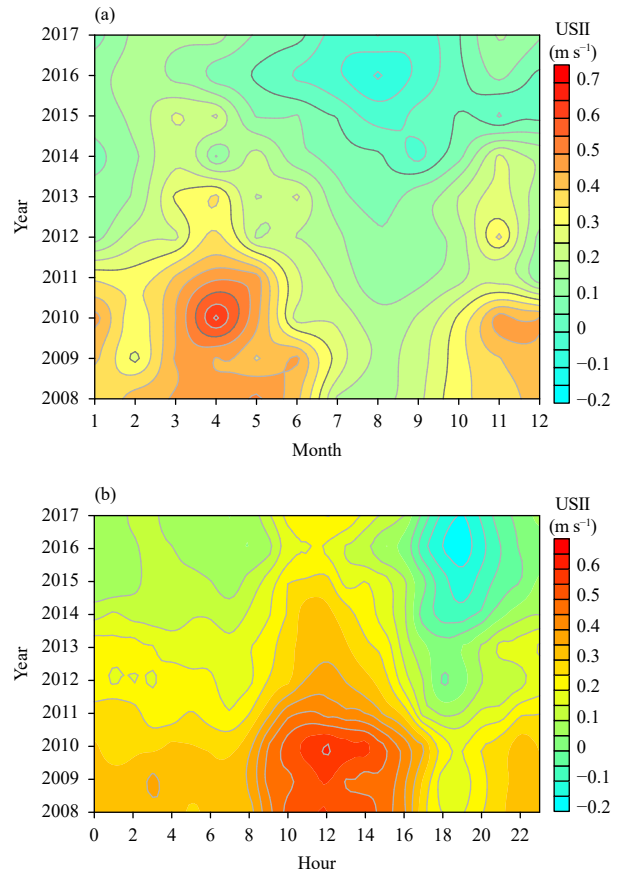


Fig. 7. (a) Month-year profile of mean USII (m s^{-1}) and (b) Hour-year profile of mean USII (m s^{-1}).

the near-surface WS (Zhou et al., 2017). In detail, the annual value of USII peaks in 2010, while it reaches the bottom in 2016. For the whole 10-year period, the inter-seasonal variability seems to be large as well. The monthly mean USII turns out to be larger in January to June and October to December, especially in spring (March to May). On the other hand, the monthly mean USII keeps low in summer (July to September). Figure 7b demonstrates that the hourly average USII changes year by year in urban areas. The diurnal changes are obvious in the whole study-year. The hourly average USIIs maintain high during the daytime and drop at the nighttime every year. However, the density and duration of the high- and low-value terms are different every year. The levels of high-value USII in 2010 and 2009 are greater, while the low-value levels of USII are more remarkable in 2016 and 2017. In addition, at any time of a day, the hourly mean value of USII decreases year by year after 2010.

Figure 8 demonstrates the hour-pentad profiles of hourly average USIIs for urban region of Beijing during the period of 2008-2017. The distribution of hourly mean USII is considerably different among the whole day and whole year. It can reach as high as 0.5 m s^{-1} during daytime (1000 to 1400 BT) in the strong USII stage of spring and winter, approximately 0.5 m s^{-1} larger than that in the evening in summer and autumn. In particular, the hourly mean USII during the daytime (0800 to 1600 BT) is obviously higher in spring. The maximum USII value

reaches 0.7 m s^{-1} around 1000 BT of the 17th pentad (middle spring), and the relatively strong USII appears at daytime during the late autumn and early winter.

It is interesting to note that there exists a negative USII stage during the evening time of late summer and early autumn, with the greatest negative values ranging from -0.2 to -0.3 m s^{-1} during early autumn (Fig. 8). The negative USII also appears in late afternoon and early evening in other seasons, particularly in early summer and winter. This phenomenon may be related to the obviously weaker background WS field and the increased UHI intensity during the specific transitional time point from summer to autumn and from afternoon and late evening (Yang et al., 2013), but the reasons need to be investigated in future. The increased UHI intensity may also leads to stronger local UHI circulation and the resulting stronger near-surface WS within the urban areas.

5. Discussion

The difference of near-surface WS between urban and rural areas has been concerned continuously. Early investigations in Beijing City are based on the observation data obtained from two meteorological towers or two weather stations for comparison, one of which is within the city and the other is outside of the city. The early studies on other regions have generally shown that WSs over city tend to be lower (e.g. Landsberg, 1956; Frederick, 1964; Graham, 1968), which is mainly attributed to the greater aerodynamic surface roughness in urban areas compared with adjacent rural regions. However, other studies indicates that UHI can make it possible to change surface WS in urban area, which enhances urban-rural temperature gradients and increases WS_u . For example, Chandler (1965) demonstrated the spatial difference of WS in and around London and found that the WS over London was greater than nearby rural sites.

In the last decade, especially in China, the latest observational evidences showed that the WS in city was decreasing more significantly than that in rural area, and in most cases, it is lower in cities than in rural regions (Liu et al., 2012; Yu et al., 2014; Wu and Wu, 2016; Bian et al., 2018). According to an analysis of the profile of upper air WS change, about one third of the decline in annual mean surface WS in mainland China on a whole is attributed to the urbanization and the change of observation environment around the current stations of the national meteorological network (Zhang et al., 2009). The simulations for flow structures in city canyon (Zhang et al., 2001) have also demonstrates that it would be profoundly affected by the height and density of buildings.

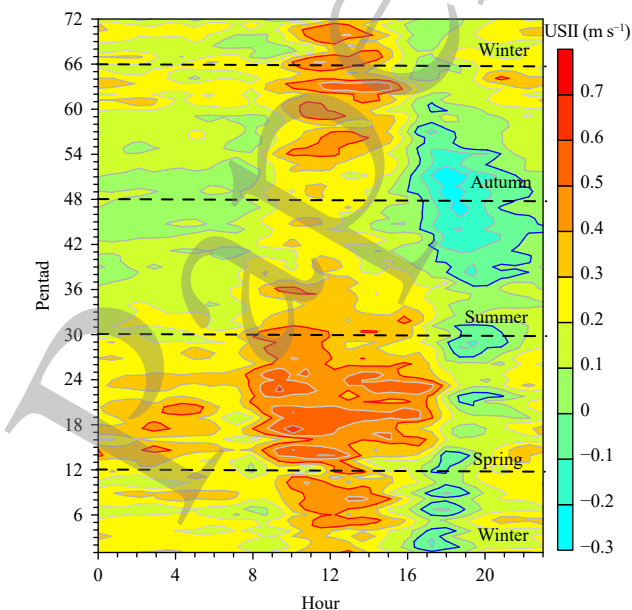


Fig. 8. Hour-pentad profile of mean USII for Beijing urban region. Blue lines represent 0 m s^{-1} isolines of mean value of USII while red lines represent 0.4 m s^{-1} isolines of mean value of USII.

Table 3. Diurnal features of USII among different seasons in Beijing city during 2008-2017(未在正文中被引用)

		Spring	Summer	Autumn	Winter
Seasonal mean value (m s^{-1})		0.49	0.31	0.31	0.41
Standard Deviation (m s^{-1})		0.12	0.10	0.13	0.09
Daily Peak	Value (m s^{-1})	0.66	0.48	0.54	0.60
	Appearance time	10 h	12 h	11 h	12 h
Daily Valley	Value (m s^{-1})	0.31	0.19	0.17	0.27
	Appearance time	20 h	20 h	18 h	18 h

If the urban buildings keep away from others with open space, or the buildings are in shorter structures, the near-surface wind would follow the direction of prevailing wind. Conversely, if the height and density of urban buildings are increased, the near-surface wind direction would be rather different from the prevailing wind, and the mean WS would be weakened. A survey shows that the height of buildings inside 5th RR of Beijing generally exceeds 15 m (Mu et al., 2019) except for the buildings around TAM in urban center, which can be explained by the nearing world largest urban square of 440 thousand m^2 . Based on a denser observational dataset in this paper, it can be concluded that WS in urban area, especially inside 5th RR, is obviously lower than in nearby rural area. Thus, it could be inferred that, during the last decades in Beijing, change in the urban environment and surface roughness accompanying the rapid urbanization has a great impact on WS_u .

Comparing Fig. 3 and Fig. 8, it is easy to find that the diurnal variations of annual mean values of WS and USII are similar. Both of the curves are in twin-peaks patterns. The maximum hourly mean value occurs at daytime in winter and spring, and the second largest value obviously appears in early morning in spring. The daily curve of hourly mean WS indicates that the WS changes remarkably during the daytime. From 0500 to 1500 BT, the hourly mean value of WS grows from 0.72 to 1.76 m s^{-1} , up more than doubled. This increase is mainly attributed to solar radiation. The strengthened solar radiation after sunrise encourages the turbulence development and the downward transmission of upper air momentum. Consequently, the WS is gradually increasing after sunrise until afternoon. On the other hand, the turbulence at night is weak and the air condition keeps calm, which contributes to lower the near-surface WS. In addition, the diurnal curve of USII presents the similar pattern, which can be partly explained by UHI effects. In urban area, nighttime UHI enhancement is common in inland temperate cities like Beijing and Shijiazhuang (Yang et al., 2013; Bian et al., 2018), which makes the atmospheric stratification less stable at night in urban areas than that in rural region. Also, the turbulence of boundary layer tends to be enhance, and it will bring the momentum from the top

downward. Thus, although the WS is weaker over urban area than in rural area, there is little difference at night due to the UHI.

The seasonal feature of USII is also a worthwhile topic to be discussed. The previous studies shows that the lowest seasonal mean UHII over Beijing is identified in spring (Yang et al., 2013), while this paper demonstrates that the strongest USII also occurs in spring. This seems to be contradictory. Actually, it is not difficult to figure out the reasons for this phenomenon. Previous studies have found that urbanization affects surface WS in two ways. One is UHI, which enhances urban-rural temperature gradient and increases WS_u . The other is surface roughness, the increasing of which acts to decrease WS_u (Klink, 1999). The surface roughness effect would dominate when the large-scale wind is stronger, which is typical in spring (Born and Johnson, 1977; Lee, 1979). Thus, the roughness has a greater impact on WS in windy seasons like spring and winter. Oppositely, if the large-scale wind is weaker, such as in autumn and summer, UHI circulation's effect on WS will be greater while the roughness influence is reduced (Li et al., 1982; Zhou and Yu, 1988). However, as a kind of local airflow, the UHI circulation is typically weak, so that the set-off is usually small. All in all, the WS in urban areas is decreased partly by the UHI circulation. Consequently, the USII is not significant in autumn and summer. Another reason for the weak wind in summer is probably attributed to varied summer precipitation, which mitigates the UHI intensity and UHI circulation. During the period of 2008-2017, for example, the annual accumulated precipitation in summer is 387 mm, almost occupying 70% of the annual total precipitation (579 mm). The weakened UHI circulation during summer may have contributed to the weak urban wind field to some extent.

However, the results presented in this paper have clearly indicated the significant urbanization effect on the weakening surface WS in urban areas. The sites selected for study includes the national observation stations such as Beijing Station (BO), Haidian Station and Chaoyang Station, which are all located in built-up areas. That is to say, the urbanization (Zhang et al., 2009; Liu et al., 2012), the increased roughness of land areas (Vautard et

al., 2010; Bichet et al., 2012) and the decrease in thermal contrast between tropical and polar regions in the context of global warming (Zhang and Ren 2003; McVicar et al., 2012) in urban areas may all influence the observational environment. As a result, the near-surface stilling facts observed from most of the stations in mainland China will also be affected as the previous studies claimed. This is important because it shows that the large-scale near-surface WS might have not declined so much as previously believed and the utilization of wind power on land will not be negatively affected by the long-term change in climate. It is very likely that at least the observed decline in surface WS on land have been caused by the locally anthropogenic shielding effect.

Furthermore, the near-surface WS is also a very important factor for the formation of haze or severe pollutant weather. Calm condition plays a positive role in generating and maintaining the haze weather, especially when the WS value keeps at lower level (Mao et al., 2018). Miao et al. (2016) studied the diurnal variation of PM_{2.5} mass concentration and found that the diurnal curve of PM_{2.5} in Beijing City has two valleys (0700 and 1600 BT), which are consistent with the USII diurnal pattern as reported in this paper. In addition, PM_{2.5} mass concentration keeps high from 0900 to 1600 BT (Miao et al., 2016), which is identical with the diurnal variation pattern of USII, especially in spring. It is likely that the pollutants emissions increase during daytime, and the relatively large USII is conducive to a high concentration of aerosols and further exacerbating the air pollution of urban areas during the period of a day.

Therefore, the analysis results obtained in this work would be important not only for understanding the WS variation between urban and rural areas and its mechanism, but also for clarifying the possible causes of the widely observed near-surface WS decline on land and for recognizing the accumulating process of air pollutants and monitoring the haze weather in the megacity.

6. Conclusions

This paper examines the climatological features of the WS and USI phenomena in Beijing urban areas by applying an hourly dataset with high quality gained from a high-density AWS network. It is concluded as follows:

(1) The annual mean values of WS in central urban areas or nearby areas tend to be small. The largest average WS values at monthly level appear in spring and winter. The hourly mean WS values change significantly within a whole day.

(2) The largest annual mean USII mostly occurs in-

side the 4th RR. With regard to the seasonal variation, the seasonal mean USIIs are stronger in spring and winter than in autumn and summer. It is closely related to the faster large-scale flow in winter and spring, resulting in the domination of surface roughness effect.

(3) Diurnal variations of annual and seasonal mean USII are similar. The annual mean USII keeps low from 1800 BT to the next morning (0700 BT). The diurnal variations, including the occurrence time of peaks, the mean value level and the general diurnal pattern, are different in each season.

(4) Both of month-year profiles and hour-year profiles of average USII at hourly level show that there are obvious two stages from 2008 to 2017, which are the period from 2008 to 2012 with larger USII values and the period from 2013 to 2017 with smaller USII values. The variation can be attributed to the urbanized level of the surroundings of reference sites.

(5) The distribution of hourly mean USII is considerable different among the whole day and whole year. It is higher during the daytime (0800 to 0600 BT) in spring than in any other hours and seasons. The maximum USII is 0.7 m s⁻¹ around 1000 BT of the 17th pentad (mid-spring). It is inferred that solar radiation plays a crucial role.

REFERENCES

- Alonso, M. S., M. R. Fidalgo, and J. L. Labajo, 2007: The urban heat island in Salamanca (Spain) and its relationship to meteorological parameters. *Climate Res.*, **34**, 39–46, doi: [10.3354/cr034039](https://doi.org/10.3354/cr034039).
- Aristidi, E., K. Agabi, M. Azouit, et al., 2005: An analysis of temperatures and wind speeds above dome C, Antarctica. *Astron. Astrophys.*, **430**, 739–746, doi: [10.1051/0004-6361:20041876](https://doi.org/10.1051/0004-6361:20041876).
- Ashrafi, K., M. Shafie-Pour, and H. Kamalan, 2009: Estimating temporal and seasonal variation of ventilation coefficients. *Int. J. Environ. Res.*, **3**, 637–644.
- Azorin-Molina, C., J. A. Guijarro, T. R. McVicar, et al., 2016: Trends of daily peak wind gusts in Spain and Portugal, 1961–2014. *J. Geophys. Res. Atmos.*, **121**, 1059–1078, doi: [10.1002/2015JD024485](https://doi.org/10.1002/2015JD024485).
- Bian, T., G. Y. Ren, and L. X. Zhang, 2018: Significant urbanization effect on decline of near-surface wind speed at Shijiazhuang station. *Climate Change Res.*, **14**, 21–30, doi: [10.12006/j.issn.1673-1719.2017.030](https://doi.org/10.12006/j.issn.1673-1719.2017.030). (in Chinese)
- Bichet, A., M. Wild, D. Folini, et al., 2012: Causes for decadal variations of wind speed over land: Sensitivity studies with a global climate model. *Geophys. Res. Lett.*, **39**, L11701, doi: [10.1029/2012GL051685](https://doi.org/10.1029/2012GL051685).
- Bornstein, R. D., and D. S. Johnson, 1977: Urban-rural wind velocity differences. *Atmos. Environ.*, **11**, 597–604, doi: [10.1016/0004-6981\(77\)90112-3](https://doi.org/10.1016/0004-6981(77)90112-3).
- Chai, Y. N., G. J. Wei, W. Hou, et al., 2018: Multi-scale eco-envir-

- omental quality evaluation method from a spatial perspective. *Chinese J. Ecol.*, **37**, 596–604, doi: [10.13292/j.1000-4890.201802.013](https://doi.org/10.13292/j.1000-4890.201802.013). (in Chinese)
- Chandler, T. J. 1965: *The Climate of London*. Hutchinson, London, 292 pp.
- Cuadrat, J. M., S. M. Vicente-Serrano, and M. Á. Saz, 2015: Influence of different factors on relative air humidity in Zaragoza, Spain. *Front. Earth Sci.*, **3**, 10, doi: [10.3389/feart.2015.00010](https://doi.org/10.3389/feart.2015.00010).
- Frederick, R. H., 1964: On the representativeness of surface wind observations using data from Nashville, Tennessee. *Int. J. Air Wat. Pollut.*, **8**, 11.未找到本条文献信息, 请核对
- Ge, Y., X. Xu, J. Li, et al., 2016: Study on the influence of urban building density on the heat island effect in Beijing. *J. Geol. Inf. Sci.*, **18**, 1698–1706, doi: [10.3724/SP.J.1047.2016.01698](https://doi.org/10.3724/SP.J.1047.2016.01698). (in Chinese)
- Graham, I. R., 1968: An analysis of turbulence statistics at fort Wayne, Indiana. *J. Appl. Meteor.*, **7**, 90–93, doi: [10.1175/1520-0450\(1968\)007<0090:AAOTSA>2.0.CO;2](https://doi.org/10.1175/1520-0450(1968)007<0090:AAOTSA>2.0.CO;2).
- Hobbins, M. T., J. A. Ramírez, and T. C. Brown, 2004: Trends in pan evaporation and actual evapotranspiration across the conterminous U.S.: Paradoxical or complementary? *Geophys. Res. Lett.*, **31**, L13503, doi: [10.1029/2004GL019846](https://doi.org/10.1029/2004GL019846).
- Hosler, C. R., 1961: Low-level inversion frequency in the contiguous United States. *Mon. Wea. Rev.*, **89**, 319–339, doi: [10.1175/1520-0493\(1961\)089<0319:LIFITC>2.0.CO;2](https://doi.org/10.1175/1520-0493(1961)089<0319:LIFITC>2.0.CO;2).
- Hou, A. Z., G. H. Ni, H. B. Yang, et al., 2013: Numerical analysis on the contribution of urbanization to wind stilling: An example over the greater Beijing metropolitan area. *J. Appl. Meteor. Climatol.*, **52**, 1105–1115, doi: [10.1175/JAMC-D-12-013.1](https://doi.org/10.1175/JAMC-D-12-013.1).
- Jiang, Y., Y. Luo, Z. C. Zhao, et al., 2010: Changes in wind speed over China during 1956–2004. *Theor. Appl. Climatol.*, **99**, 421–430, doi: [10.1007/s00704-009-0152-7](https://doi.org/10.1007/s00704-009-0152-7).
- Klink, K., 1999: Trends in mean monthly maximum and minimum surface wind speeds in the coterminous United States, 1961 to 1990. *Climate Res.*, **13**, 193–205, doi: [10.3354/cr013193](https://doi.org/10.3354/cr013193).
- Landsberg, H. E., 1956: The climate of towns. *Man's Role in Changing the Face of the Earth*, W. L. Thomas, Ed., University of Chicago Press, Chicago, Illinois, 584–606.
- Lee, D. O., 1979: The influence of atmospheric stability and the urban heat island on urban-rural wind speed differences. *Atmos. Environ.*, **13**, 1175–1180, doi: [10.1016/0004-6981\(79\)90042-8](https://doi.org/10.1016/0004-6981(79)90042-8).
- Li, Y. Y., S. H. Qu, and M. Y. Zhou, 1982: Analysis of flow melts in Beijing area. *Acta Sci. Circumstant.*, **2**, 351–357. (in Chinese)
- Li, Z., Z. W. Yan, K. Tu, et al., 2011: Changes in Wind Speed and Extremes in Beijing during 1960–2008 based on homogenized observations. *Adv. Atmos. Sci.*, **28**, 408–420, doi: [10.1007/s00376-010-0018-z](https://doi.org/10.1007/s00376-010-0018-z).
- Liu, X. F., X. H. Liang, G. Y. Ren, et al., 2012: Impact of the observational environment change on surface wind speed in China. *Plateau Meteor.*, **31**, 1645–1652. (in Chinese)
- Liu, Y., S. G. Wang, K. Z. Shang, et al., 2002: Time-Space changing character of low-level wind in Lanzhou city and its correlation with air pollution. *Plateau Meteor.*, **21**, 322–326, doi: [10.3321/j.issn:1000-0534.2002.03.015](https://doi.org/10.3321/j.issn:1000-0534.2002.03.015). (in Chinese)
- Lynch, A. H., J. A. Curry, R. D. Brunner, et al., 2004: Toward an integrated assessment of the impacts of extreme wind events on Barrow, Alaska. *Bull. Am. Meteor. Soc.*, **85**, 209–222, doi: [10.1175/BAMS-85-2-209](https://doi.org/10.1175/BAMS-85-2-209).
- Mao, Z. C., J. H. Ma, Y. H. Qu, et al., 2018: Relationships between air quality and meteorological conditions in Shanghai in 2015. *J. Meteor. Environ.*, **34**, 52–60, doi: [10.3969/j.issn.1673-503X.2018.02.007](https://doi.org/10.3969/j.issn.1673-503X.2018.02.007). (in Chinese)
- McVicar, T. R., M. L. Roderick, R. J. Donohue, et al., 2012: Global review and synthesis of trends in observed terrestrial near-surface wind speeds: Implications for evaporation. *J. Hydrol.*, **416–417**, 182–205, doi: [10.1016/j.jhydrol.2011.10.024](https://doi.org/10.1016/j.jhydrol.2011.10.024).
- Miao, L., X. N. Liao, and Y. C. Wang, 2016: Diurnal variation of PM_{2.5} mass concentration in Beijing and influence of meteorological factors based on long term date. *Environ. Sci.*, **37**, 2836–2846, doi: [10.13227/j.hjcx.2016.08.003](https://doi.org/10.13227/j.hjcx.2016.08.003). (in Chinese)
- Mu, Q. C., S. G. Miao, Y. W. Wang, et al., 2019: Evaluation of employing local climate zone classification for mesoscale modelling over Beijing metropolitan area. *Meteor. Atmos. Phys.* doi: [10.1007/s00703-019-00692-7](https://doi.org/10.1007/s00703-019-00692-7).
- Mu, X. D., H. P. Liu, and X. J. Xue, 2012: Urban growth in Beijing from 1984 to 2007 as gauged by remote sensing. *J. Beijing Normal Univ. (Nat. Sci.)*, **48**, 81–85. (in Chinese)
- Oke, T. R., 1988: The urban energy balance. *Prog. Phys. Geogr.*, **12**, 471–508, doi: [10.1177/030913338801200401](https://doi.org/10.1177/030913338801200401).
- Peng, Z., and F. Hu, 2006: A study of the influence of urbanization of Beijing on the boundary wind structure. *Chinese J. Geophys.*, **49**, 1608–1615, doi: [10.3321/j.issn:0001-5733.2006.06.005](https://doi.org/10.3321/j.issn:0001-5733.2006.06.005). (in Chinese)
- Pielke, R. A., G. Marland, R. A. Betts, et al., 2002: The influence of land-use change and landscape dynamics on the climate system: relevance to climate-change policy beyond the radiative effect of greenhouse gases. *Philos. Trans. Roy. Soc. A: Math. Phys. Eng. Sci.*, **360**, 1705–1719, doi: [10.1098/rsta.2002.1027](https://doi.org/10.1098/rsta.2002.1027).
- Pirazzoli, P. A., and A. Tomasin, 2003: Recent near-surface wind changes in the central Mediterranean and Adriatic areas. *Int. J. Climatol.*, **23**, 963–973, doi: [10.1002/joc.925](https://doi.org/10.1002/joc.925).
- Ren, G. Y., and Y. Q. Zhou, 2014: Urbanization effect on trends of extreme temperature indices of national stations over mainland China, 1961–2008. *J. Climate*, **27**, 2340–2360, doi: [10.1175/JCLI-D-13-00393.1](https://doi.org/10.1175/JCLI-D-13-00393.1).
- Ren, G. Y., J. Guo, M. Z. Xu, et al., 2005: Climate changes of China's mainland over the past half Century. *Acta Meteor. Sinica*, **63**, 942–956. (in Chinese)
- Ren, G. Y., Z. Y. Chu, Z. H. Chen, et al., 2007: Implications of temporal change in urban heat island intensity observed at Beijing and Wuhan stations. *Geophys. Res. Lett.*, **34**, L05711, doi: [10.1029/2006GL027927](https://doi.org/10.1029/2006GL027927).
- Ren, Y. Y., and G. Y. Ren, 2011: A remote-sensing method of selecting reference stations for evaluating urbanization effect on surface air temperature trends. *J. Climate*, **24**, 3179–3189, doi: [10.1175/2010JCLI3658.1](https://doi.org/10.1175/2010JCLI3658.1).
- Roderick, M. L., L. D. Rotstayn, G. D. Farquhar, et al., 2007: On the attribution of changing pan evaporation. *Geophys. Res. Lett.*, **34**, L17403, doi: [10.1029/2007GL031166](https://doi.org/10.1029/2007GL031166).
- Shapiro, A., and E. Fedorovich, 2018: An analytical model of an urban heat island circulation in calm conditions. *Environ. Flu-*

- id Mech.*, **19**, 111–135, doi: [10.1007/s10652-018-9621-9](https://doi.org/10.1007/s10652-018-9621-9).
- Torralba, V., F. J. Doblas-Reyes, and N. Gonzalez-Reviriego, 2017: Uncertainty in recent near-surface wind speed trends: A global reanalysis intercomparison. *Environ. Res. Lett.*, **12**, 114019, doi: [10.1088/1748-9326/aa8a58](https://doi.org/10.1088/1748-9326/aa8a58).
- Tuller, S. E., 2004: Measured wind speed trends on the west coast of Canada. *Int. J. Climatol.*, **24**, 1359–1374, doi: [10.1002/joc.1073](https://doi.org/10.1002/joc.1073).
- Turner, J., S. R. Colwell, G. J. Marshall, et al., 2005: Antarctic climate change during the last 50 years. *Int. J. Climatol.*, **25**, 279–294, doi: [10.1002/joc.1130](https://doi.org/10.1002/joc.1130).
- Unger, J., 1996: Heat island intensity with different meteorological conditions in a medium-sized town: Szeged, Hungary. *Theor. Appl. Climatol.*, **54**, 147–151, doi: [10.1007/bf00865157](https://doi.org/10.1007/bf00865157).
- Vautard, R., J. Cattiaux, P. Yiou, et al., 2010: Northern hemisphere atmospheric stilling partly attributed to an increase in surface roughness. *Nat. Geosci.*, **3**, 756–761, doi: [10.1038/ngeo979](https://doi.org/10.1038/ngeo979).
- Wu, X., and W. Q. Wu, 2016: Urban-rural differences in the probability distribution of surface wind speed in Nanjing. *Climatic Environ. Res.*, **21**, 134–140, doi: [10.3878/j.issn.1006-9585.2015.15026](https://doi.org/10.3878/j.issn.1006-9585.2015.15026). (in Chinese)
- Xu, M., C. P. Chang, C. B. Fu, et al., 2006: Steady decline of East Asian monsoon winds, 1969–2000: Evidence from direct ground measurements of wind speed. *J. Geophys. Res. Atmos.*, **111**, D24111, doi: [10.1029/2006JD007337](https://doi.org/10.1029/2006JD007337).
- Yang, D. Q., S. Ishida, B. E. Goodison, et al., 1999: Bias correction of daily precipitation measurements for Greenland. *J. Geophys. Res. Atmos.*, **104**, 6171–6181, doi: [10.1029/1998JD200110](https://doi.org/10.1029/1998JD200110).
- Yang, P., G. Y. Ren, and W. D. Liu, 2013: Spatial and temporal characteristics of Beijing urban heat island intensity. *J. Appl. Meteor. Climatol.*, **52**, 1803–1816, doi: [10.1175/jamc-d-12-0125.1](https://doi.org/10.1175/jamc-d-12-0125.1).
- Yang, P., G. Y. Ren, and W. Hou, 2017: Temporal-spatial patterns of relative humidity and the urban dryness island effect in Beijing City. *J. Appl. Meteor. Climatol.*, **56**, 2221–2237, doi: [10.1175/JAMC-D-16-0338.1](https://doi.org/10.1175/JAMC-D-16-0338.1).
- Yang, P., W. D. Liu, J. Q. Zhong, et al., 2011: Evaluating the quality of temperature measured at Automatic Weather Stations in Beijing. *J. Appl. Meteor. Sci.*, **22**, 706–715, doi: [10.3969/j.issn.1001-7313.2011.06.008](https://doi.org/10.3969/j.issn.1001-7313.2011.06.008). (in Chinese)
- Yang, P., Z. N. Xiao, and M. S. Ye, 2016: Cooling effect of urban parks and their relationship with urban heat islands. *Atmos. Ocean. Sci. Lett.*, **9**, 298–305, doi: [10.1080/16742834.2016.1191316](https://doi.org/10.1080/16742834.2016.1191316).
- Yao, H. R., and D. L. Li, 2016: The interannual variation of wind speed in the Tibetan Plateau in spring and its response to global warming during 1971–2012. *Acta Meteor. Sinica*, **74**, 60–75, doi: [10.11676/qxxb2016.006](https://doi.org/10.11676/qxxb2016.006). (in Chinese)
- Yu, H. M., Y. Q. Xu, and H. L. Zhang, 2014: The impact on wind speed trend of urbanization at Heilongjiang province. *Acta Energ. Sol. Sinica*, **35**, 1797–1802, doi: [10.3969/j.issn.0254-0096.2014.09.037](https://doi.org/10.3969/j.issn.0254-0096.2014.09.037). (in Chinese)
- Zhang, A. Y., G. Y. Ren, J. Guo, et al., 2009: Change trend analyses on upper-air wind speed over China in past 30 years. *Plateau Meteor.*, **28**, 680–687. (in Chinese)
- Zhang, L., and G. Y. Ren, 2003: Change in dust storm frequency and the climatic controls in northern China. *Acta Meteor. Sinica*, **61**, 744–750, doi: [10.11676/qxxb2003.075](https://doi.org/10.11676/qxxb2003.075). (in Chinese)
- Zhang, N., W. M. Jiang, and F. Hu, 2001: Simulations for flow structures in city canyon with k-ε turbulence energy closure scheme. *Acta Aerodyn. Sinica*, **19**, 296–301, doi: [10.3969/j.issn.0258-1825.2001.03.008](https://doi.org/10.3969/j.issn.0258-1825.2001.03.008). (in Chinese)
- Zhang, Z. B., Y. Yang, X. P. Zhang, et al., 2014: Wind speed changes and its influencing factors in southwestern China. *Acta Ecol. Sinica*, **34**, 471–481, doi: [10.5846/stxb201305141051](https://doi.org/10.5846/stxb201305141051). (in Chinese)
- Zheng, Z. F., and G. Y. Ren, 2017: Effects of gauge under-catch on precipitation observation and long-term trend estimates in Beijing area. *Adv. Water Sci.*, **28**, 662–670, doi: [10.14042/j.cnki.32.1309.2017.05.003](https://doi.org/10.14042/j.cnki.32.1309.2017.05.003). (in Chinese)
- Zhou, B. Y., F. Zheng, and J. Zhu, 2017: Analysis of the interannual variations and influencing factors of wind speed anomalies over the Beijing-Tianjin-Hebei region. *Atmos. Ocean. Sci. Lett.*, **10**, 312–318, doi: [10.1080/16742834.2017.1327301](https://doi.org/10.1080/16742834.2017.1327301).
- Zhou, S. Z., and B. X. Yu, 1988: Shanghai urban influences on wind velocity. *J. East China Normal Univ. (Nat. Sci.)*, **3**, 68–76. (in Chinese) (请核对卷号信息)